Effects of Lévy noise in aperiodic stochastic resonance

2007 J. Phys. A: Math. Theor. 40 7175

(http://iopscience.iop.org/1751-8121/40/26/005)

J. Phys. A: Math. Theor. **40** (2007) 7175–7185 doi:10.1088/1751-8113/40/26/005

Effects of Lévy noise in aperiodic stochastic resonance

Lingzao Zeng, Ronghao Bao and Bohou Xu

Department of Mechanics, State Key Laboratory of Fluid Power Transmission and Control, Zhejiang University, Hangzhou 310027, People's Republic of China

E-mail: xubohou@zju.edu.cn and brh@zju.edu.cn

Received 25 November 2006, in final form 9 April 2007
Published 12 June 2007
Online at stacks.iop.org/JPhysA/40/7175

Abstract

We present a Grünwald–Letnikov implicit finite difference method to solve the space-fractional Fokker–Planck equation with natural boundary condition. Then the properties of aperiodic stochastic resonance in the presence of Lévy noise are investigated in theory and tested by simulation. It is shown that aperiodic stochastic resonance does occur in the presence of Lévy noise, but is reduced by the lower Lévy index α. With the optimal system parameters, the probability of detection error decreases with the decrease of α. Therefore, the performance of a bistable system is improved by the lower index α of Lévy noise.

PACS numbers: 05.40.−a, 02.50.−r

1. Introduction

In recent years, anomalous processes have attracted much attention due to their ubiquity. As a result of the invalidity of the central limit theory, traditional diffusion theorems cannot describe many complex systems and phenomenons, where the distributions of random variables exhibit in power law [1–5]. These processes are usually classified as subdiffusion and superdiffusion, which correspond to the long temporal rests and the long spatial jumps respectively. They can be described by a fractional Fokker–Planck equation(FFPE) derived from continuous time random walk with power-law distributed waiting time or a jumping length, i.e., $\psi(t) \sim t^{-1-\alpha}$ or $\lambda(|x|) \sim |x|^{-1-\alpha}$. FFPE is usually employed as a convenient tool to describe the nonequilibrium dynamics of anomalous diffusion in an external potential. In corresponding to processes with long waiting time, the traditional Fokker–Planck equation (FPE) is generalized into a time-fractional derivative form, or into a space-fractional form for long jumping processes. As a model of superdiffusion and a generation from Gaussian diffusion processes, Lévy flights has been investigated vastly recently. For a recent review, one may refer to [6].

Stochastic resonance (SR) is a counterintuitive phenomenon. Under some conditions, noise plays an active role in the system output [7–9]. Investigations have been carried out to analyse the potentialities of stochastic resonance in signal processing [10–13]. In the binary signal processing, the performance of a bistable detector is compared with a matched filter in [14]. It is shown that under the condition of desynchronization, the bistable detector provides a competitive or even better performance than the matched filter. Recently, some work has been done to investigate the quantities which are related to SR in anomalous processes. In the subdiffusive case, the linear response theory in the subdiffusive bistable system has been discussed in [15]. The effects of long-tailed waiting time in aperiodic stochastic resonance (ASR) are studied in [16]. While in the superdiffusive case, it is shown that the periodic SR phenomenon still occurs in the presence of Lévy noise [17]. Some other work was done to show the anomalous properties of Lévy flights in an external potential, such as the confinement and multimodality [18, 19]. Despite the universality of superdiffusion, the effects of Lévy noise in ASR have not been investigated. It is worthwhile studying the cooperative effects between the external potential and Lévy noise in ASR.

In this paper, we focus on the nonequilibrium dynamics of a bistable system excited by the Lévy noise and binary signal. It is organized as follows. As analytical solutions of FFPE with a nonlinear potential are not available, in section 2, an implicit Grünwald–Letnikov finite difference method is presented. Then the evolutions of probability distribution are obtained. In section 3, we propose a quantity known as the dynamical probability of the detection error P_{err} to quantify the performance of a bistable receiver. Then the anomalous properties of ASR in the presence of Lévy noise are investigated. Two kinds of ASR, including adding noise intensity and tuning system parameters, are discussed. The theoretical prediction and numerical simulation results are discussed. Finally, the conclusions are given in section 4.

2. Fractional Fokker–Planck equation and the solutions

We consider the Langevin equation driven by Lévy noise [20, 21]

$$\frac{\mathrm{d}x}{\mathrm{d}t} = F(x) + \Gamma_\alpha(t), \tag{1}$$

where $F(x) = -\frac{\mathrm{d}U(x)}{\mathrm{d}x}$ is the external force with potential $U(x)$, $\Gamma_\alpha(t)$ is stationary white Lévy noise with index $\alpha(1 < \alpha < 2)$. In Fourier space, the characteristic function $p_\alpha(k)$ of Lévy distribution is defined as

$$p_\alpha(k) = \exp(-D|k|^\alpha), \tag{2}$$

where the parameter D characterizes the intensity of the noise. The probability density $P_\alpha(x)$ has an asymptotic power law form $P_\alpha(x) \sim |x|^{-1-\alpha}$ [22]. In the limit case $\alpha = 2$, the Gaussian noise is recovered, and (1) leads to the normal diffusion in the external potential, which has been studied for a long history.

The equivalent Fokker–Planck equation, which describes the evolution of probability, has the fractional derivative form as follows [20, 21]:

$$\frac{\partial}{\partial t}P(x,t) = -\frac{\partial}{\partial x}[F(x)P(x,t)] + D\frac{\partial^\alpha P(x,t)}{\partial |x|^\alpha}. \tag{3}$$

The Riesz space-fractional derivative $\partial^\alpha/\partial|x|^\alpha$ is defined through the Weyl fractional operator [23] as

$$\frac{\partial^\alpha P(x,t)}{\partial|x|^\alpha} = -\frac{D_+^\alpha P(x,t) + D_-^\alpha P(x,t)}{2\cos(\pi\alpha/2)}, \tag{4}$$

where

$$D_+^\alpha P(x,t) = \frac{1}{\Gamma(2-\alpha)}\frac{\mathrm{d}^2}{\mathrm{d}^2 x}\int_{-\infty}^{x}\frac{P(\eta,t)\,\mathrm{d}\eta}{(x-\eta)^{\alpha-1}}, \tag{5}$$

and

$$D_{-}^{\alpha}P(x,t) = \frac{1}{\Gamma(2-\alpha)}\frac{\mathrm{d}^2}{\mathrm{d}^2 x}\int_x^{+\infty}\frac{P(\eta,t)\,\mathrm{d}\eta}{(\eta-x)^{\alpha-1}}, \tag{6}$$

or implicitly defined in Fourier space [23]

$$F\left\{D_{\pm}^{\alpha}P(x,t)\right\} = (\mp ik)^{\alpha}P(k,t), \tag{7}$$

where F denotes the Fourier transform. As shown in the convolution form in (5) and (6), the evolution of probability behaves strongly non-locally in space, which is introduced by the long tailed character of Lévy noise.

We employ the Grünwald–Letnikov scheme [24, 25] to numerically solve the spatial FFPE (3). Define the $t_n = n\Delta t$ as the integration time $0 \leqslant t_n \leqslant T$, and Δx as the spatial grid size, $\Delta x = (x_{\text{high}} - x_{\text{low}})/N$, hence the domain is discretized as $x_j = x_{low} + j\Delta x$, for $j = 0, \ldots, N$. The interval $[x_{\text{low}}, x_{\text{high}}]$ can be determined so that all the probability outside the domain can be omitted. Define $P_j^n = P(x_j, t_n)$, then the Riesz fractional derivative term in (3) can be represented in the following discretization form [6]:

$$\frac{\partial^{\alpha}P_j^n}{\partial|x|^{\alpha}} = -\frac{1}{2(\Delta x)^{\alpha}\cos(\pi\alpha/2)}\sum_{k=0}^{J}C_k\left(P_{j+1-k}^n + P_{j-1+k}^n\right), \tag{8}$$

where

$$C_k = (-1)^k\binom{\alpha}{k} = (-1)^k\frac{\Gamma(\alpha+1)}{\Gamma(k+1)\Gamma(\alpha-k+1)}. \tag{9}$$

In the special case $\alpha = 2$, the standard difference method for the second-order derivative is recovered. Using an implicit finite difference approximation, we express (3) in the following form:

$$\begin{aligned}\frac{P_j^{n+1} - P_j^n}{\Delta t} &= -F'(x_j)P_j^{n+1} - F(x_j)\frac{P_{j+1}^{n+1} - P_{j-1}^{n+1}}{2\Delta x}\\ &\quad -\frac{D}{2(\Delta x)^{\alpha}\cos(\pi\alpha/2)}\sum_{k=0}^{J}C_k\left(P_{j+1-k}^{n+1} + P_{j-1+k}^{n+1}\right).\end{aligned} \tag{10}$$

We move all terms in (10) at the time level $n+1$ on the-left side of the equation and level n on the right-side; (10) can be written in the following form:

$$[1 + \Delta t \cdot F'(x_j)]P_j^{n+1} + \frac{\beta}{2}F(x_j)P_{j+1}^{n+1} - \frac{\beta}{2}F(x_j)P_{j-1}^{n+1} + \sum_{k=0}^{J}M\cdot C_k\left(P_{j+1-k}^{n+1} + P_{j-1+k}^{n+1}\right) = P_j^n, \tag{11}$$

where $\beta = \frac{\Delta t}{\Delta x}$, $M = \frac{D\Delta t}{2(\Delta x)^{\alpha}\cos(\pi\alpha/2)}$. Equation (11) can be written in the matrix form and solved numerically. We consider the boundary condition $P_0 = P_N = 0$, then (11) can be expressed as follows:

$$[T]\{P\}^{n+1} = \{P\}^n, \tag{12}$$

where

$$T_{i,j} = \begin{cases} 1 + \Delta t\cdot F'(x_i) + 2MC_1, & \text{for} \quad i = j,\\ \frac{\beta}{2}F(x_i) + M(C_0 + C_2), & \text{for} \quad j = i+1,\\ -\frac{\beta}{2}F(x_i) + M(C_0 + C_2), & \text{for} \quad j = i-1,\\ MC_{j-i+1}, & \text{for} \quad j \geqslant i+2,\\ MC_{i-j+1}, & \text{for} \quad j \leqslant i-2, \end{cases} \tag{13}$$

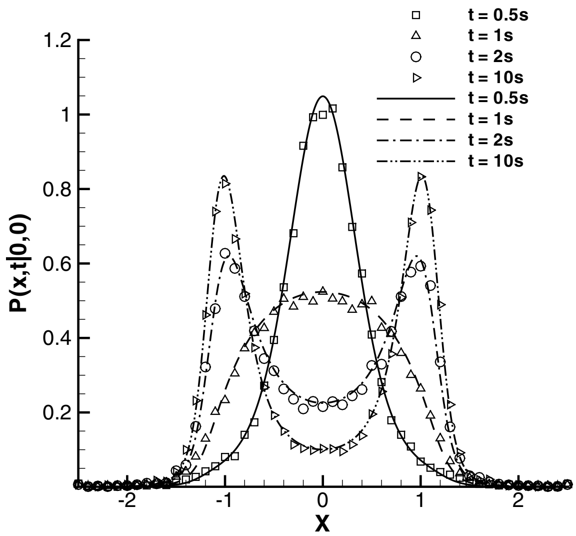

Figure 1. The evolution of $P(x, t|0, 0)$ with parameters $a = 1, b = 1, D = 0.2$ and Lévy index $\alpha = 1.5$. The lines are the numerical results by the Grünwald–Letnikov implicit difference method, the symbols are results from Monte Carlo experiments.

for $i = 1, \ldots, N-1$, $j = 1, \ldots, N-1$, and $\{P\} = [P_1, P_2, \ldots, P_{N-1}]^T$. The sum of P_i satisfies the normalization condition

$$\sum_{k=1}^{N-1} P_k = \frac{1}{\Delta x}. \tag{14}$$

With the above method, the numerical solution can be obtained by solving the linear equations (12) iteratively.

Choosing parameters as $D = 0.2, U(x) = -0.5x^2 + 0.25x^4$, with initial condition $P(x, 0) = \delta(x)$, the evolutions of probability density are shown in figures 1–3 for $\alpha = 1.5, \alpha = 1.75$ and $\alpha = 2$ by lines respectively. After the time $t = 10s$, All the systems preserve the states, and therefore, can be regarded as stable. The stationary distribution of normal diffusion ($\alpha = 2$) is well known as Maxwell distribution.

To test the validity of the numerical method, we can simulate (1) through the following discrete form:

$$x_{n+1} = x_n + F(x_n)\Delta t + \Delta t^{1/\alpha}\xi, \tag{15}$$

where ξ is Lévy distributed random variable with intensity D and index α. Using the algorithm presented by McCulloch [26] to generate Lévy white noise, we carry out the Monte Carlo experiment for 20 000 times, then divide the interval into parts. By counting the number of the points in each parts, we can get the probability density from simulation. The Monte Carlo results are plotted in figures 1–3 with symbols. It is shown that the simulation results have a good agreement with the numerical results.

As shown in these figures, with the decrease of the Lévy index α, the stationary distribution exhibits a larger deviation from Maxwell distribution. In a quartic bistable potential, a sharper stationary distribution is induced by the lower α.

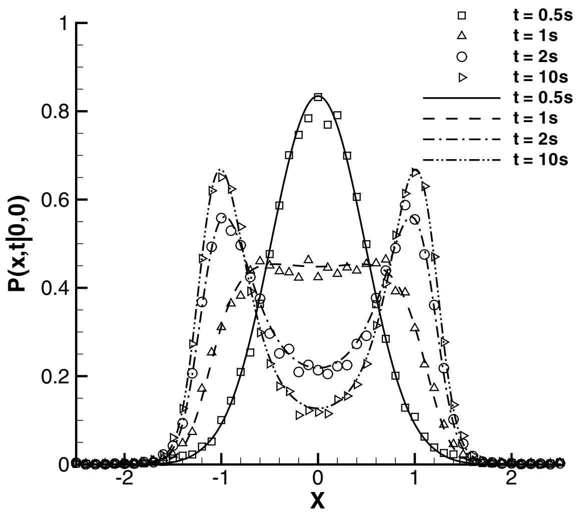

Figure 2. The evolution of $P(x, t|0, 0)$ with parameters $a = 1$, $b = 1$, $D = 0.2$ and Lévy index $\alpha = 1.75$. The lines are the numerical results by the Grünwald–Letnikov implicit difference method, the symbols are results from Monte Carlo experiments.

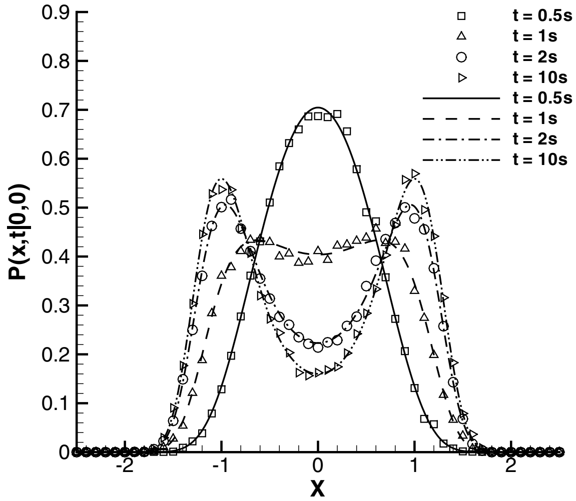

Figure 3. The evolution $P(x, t|0, 0)$ with parameters $a = 1$, $b = 1$, $D = 0.2$ of normal diffusion ($\alpha = 2$). The lines are the numerical results by the Grünwald–Letnikov implicit difference method; the symbols are results from Monte Carlo experiments.

3. Aperiodic stochastic resonance in the presence of Lévy noise

In this section, we consider the binary signal processing via a bistable system in the presence of Lévy noise. In contrast to the quantity signal-to-noise ratio (SNR) in the theory of periodic SR, here we define the probability of detection error P_{err} to measure the system performance.

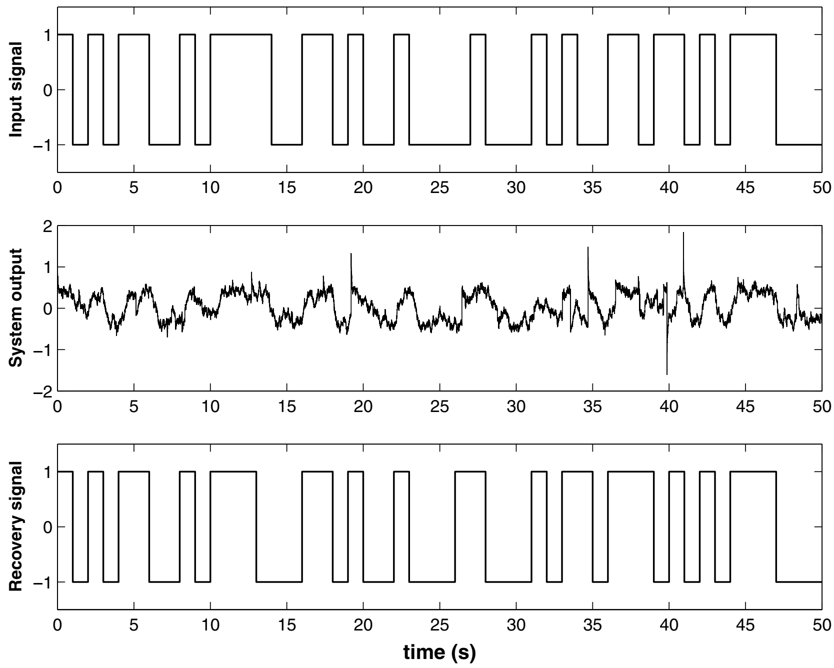

Figure 4. From top to bottom, the input binary signal, the system output and recovery signal from detection.

P_{err} characterizes the ability of the bistable receiver to detect the binary inputs. Assuming the bit time is T_b and the amplitude of the signal is h, the two hypotheses are

$$F(x) = ax - bx^3 + h(t), \qquad \begin{cases} \text{case 1}: & h(t) = h, \\ \text{case 2}: & h(t) = -h. \end{cases} \tag{16}$$

A decision is made at every duration T_b to detect the binary signal according to the output of the system $x(t)$ and the decision threshold x_{th}:

$$\begin{cases} h(t) = h, & \text{if} \quad x(t) > x_{th} \\ h(t) = -h, & \text{if} \quad x(t) < x_{th}. \end{cases} \tag{17}$$

Assume the signal h and $-h$ are statistically independent and equiprobable, $P(h) = P(-h) = 0.5$. Due to the symmetry, the threshold is chosen as $x_{th} = 0$, P_{err} can be defined as [14]

$$P_{error} = \sum_{i=1}^{+\infty} \frac{1}{2^i} \int_{-\infty}^{0} P(x, i \cdot T_b|h)\,dx. \tag{18}$$

$P(x, t|h)$ has the initial condition $P(x, 0|h) = P_0(x|-h)$, where $P_0(x|-h)$ is the stationary distribution of the system output modulated by signal $-h$.

To illustrate the detection process, we choose the parameters as $a = 1, b = 25$. The binary signal is with bit time $T_b = 1s$ and amplitude $h = 1$. The parameters of Lévy noise are $\alpha = 1.75$ and $D = 0.2$. The input binary signal, the system output and the signal recovered from detection are plotted in figure 4. Since the system output $x > 0$ at time $t = 35$ s, the signal recovered from detection is $h = 1$ during the period from $t = 34$ s to $t = 35$ s, which is an error detection.

By assuming that the parameters of the bistable system are fixed as $a = 1$ and $b = 25$, and the binary signal has amplitude $h = 0.1$ and bit time $T_b = 3$ s, we tune the intensity of Lévy

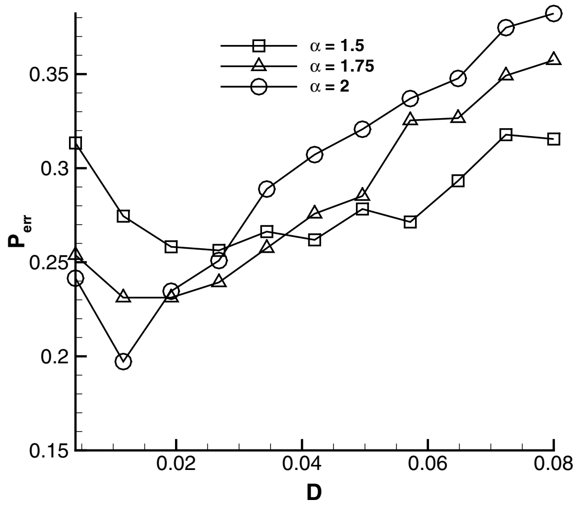

Figure 5. The simulated P_{err} versus noise intensity D with system parameters $a = 1$ and $b = 25$. The signal is with amplitude $h = 0.1$ and bit time $T_b = 3s$.

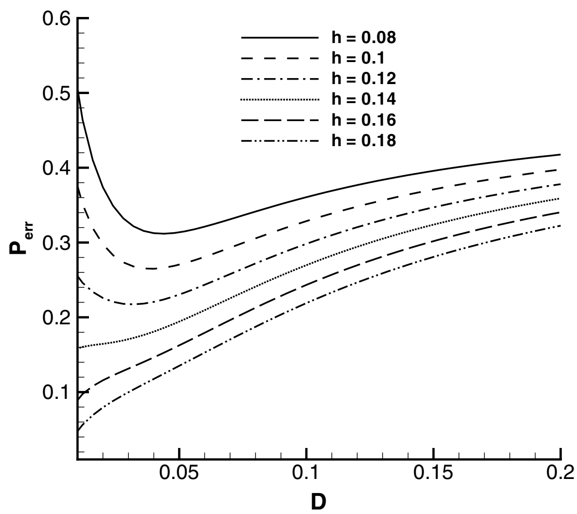

Figure 6. The theoretical P_{err} versus noise intensity D with system parameters $a = 1$, $b = 25$, bit time $T_b = 3$ s, Levy noise index $\alpha = 1.5$ for different signal amplitude h.

noise D ranging from 0.004 to 0.08. The P_{err} for different index α of Lévy noise obtained from simulation is plotted in figure 5. It is shown that P_{err} decreases with the increase of Lévy noise intensity D at first, then increases, i.e., with the intensity D at a certain range; Lévy noise helps the bistable receiver transmit the binary signal more effectively with increasing noise intensity. This is the typical character of SR.

To investigate the effects of the signal amplitude h and the index α of Lévy noise on P_{err}, we get the theoretical P_{err} with different h and α by the Grünwald–Letnikov implicit finite difference method, as shown in figures 6–8. Note that the stationary distribution $P_0(x)$ is no longer Maxwell distribution and cannot be analytically calculated [27], we employ the

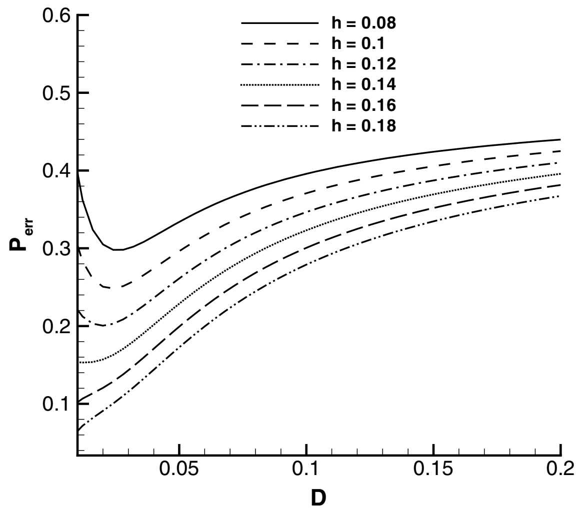

Figure 7. The theoretical P_{err} versus noise intensity D with system parameters $a = 1$, $b = 25$, bit time $T_b = 3$ s, Levy noise index $\alpha = 1.75$ for different signal amplitude h.

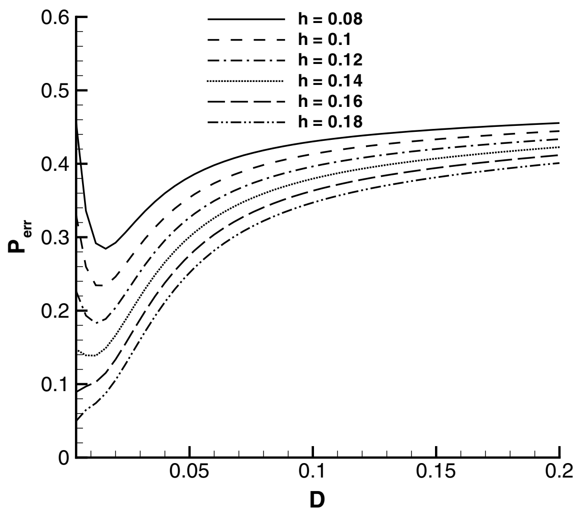

Figure 8. The theoretical P_{err} versus intensity D of Gaussian noise ($\alpha = 2$) with system parameters $a = 1$, $b = 25$, bit time $T_b = 3$ s, for different signal amplitude h.

above finite difference method to numerically get the distribution function at a long enough time, which can approximate the stationary solution. When the index α is fixed, with the increase of h, the ASR phenomenon is reduced, and disappears at a large value of h. It is also shown that the lower index α reduces the ASR phenomena. For instance, at the binary signal amplitude level $h = 0.14$, ASR still occurs with $\alpha = 2$ (Gaussian noise), almost disappears with $\alpha = 1.75$. With $\alpha = 1.5$, P_{err} obviously increases with the increasing D.

In the foregoing discussions, the noise intensity D is tunable, and the SR is called noise-induced SR. Usually, the noise intensity D and the index α are fixed, our goal is to tune the system parameters to get the lowest P_{err}, and the corresponding parameters give rise to

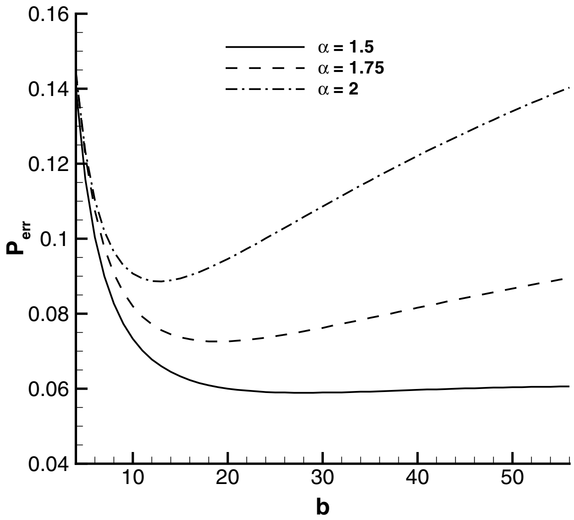

Figure 9. The theoretical values of P_{err} versus parameter b with parameters $D = 0.2, a = 1,$ $h = 1, T_b = 1$ s.

parameter-induced SR (PSR). A detailed comparison between adding Gaussian noise and tuning system parameters is discussed in [28]. With the fixed system parameter $a = 1$ and the tunable parameter b, the signal amplitude $h = 1$, bit time $T_b = 1s$, the noise intensity $D = 0.2$, we get P_{err} for a different index α, as plotted in figure 9. It is shown that, with the increase of b, P_{err} decreases at first, then increases. The optimal b, at which P_{err} is minimum, give rise to PSR in the presence of Lévy noise. In the presence of Gaussian noise ($\alpha = 2$), this optimal value is obviously about $b = 11$. With the decrease of α, this non-monotonic behaviour of P_{err} versus b fades away. When $\alpha = 1.5$, P_{err} increases very slowly after b reaches the optimal value. We also note that the optimal value of b increases with the decrease of α, i.e., $b = 11, b = 19$ and $b = 25$ for $\alpha = 2, \alpha = 1.75$ and $\alpha = 1.5$ respectively. According to the parameter-induced ASR theory in the Gaussian noise case [13], larger b leads to a larger system response speed. The system response speed λ_1, defined by the first positive eigenvalue of FPE [29] (i.e., (3) in the case $\alpha = 2$), characterizes the speed of the system relaxes to its stationary state. The system response speed must be large enough so that the output of the system can follow the varying signal. However, a too large system's response speed leads to a high P_{err}. Hence there is an optimal system response speed. Although the eigenvalue problems in spatial FFPE are not known so far, the eigenvalue of traditional FPE can characterize the relaxation speed in some sense due to the common exponential relaxation mode. Therefore, in the design of the optimal bistable receiver in the presence of Lévy noise, when the index α is determined, the optimal system response speed must be chosen as larger than the Gaussian case with the same noise intensity.

Figure 9 also shows that with respective optimal system parameters, lower α leads to the lower P_{err}. This result is remarkable because that, with the same noise intensity, the optimal system in the presence of Lévy noise behaves better than in the presence of Gaussian noise. The mechanism is related to the anomalous relaxation and can be explained as follows. The fatter tail of distribution on the error probability integration domain $(-\infty, 0)$ results in the larger P_{err}. The probability density $P(x, T_b|h)$ of different α is shown in figure 10. It is shown that, the shorter tail of output on the domain $x < 0$ is introduced by the longer tail of Lévy noise, i.e., lower α.

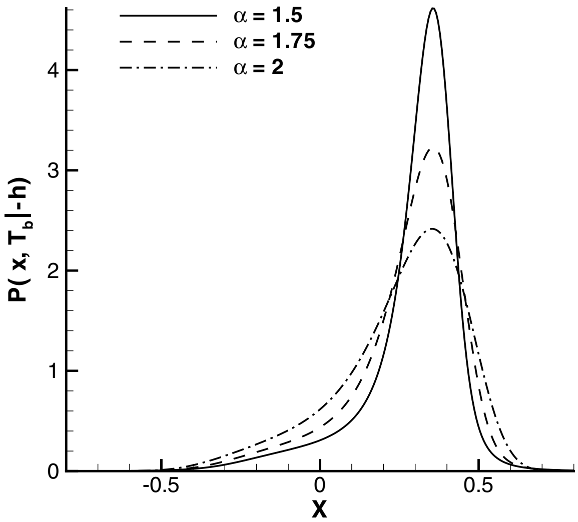

Figure 10. The probability density at time $T_b = 1$ s with parameters $D = 0.2, a = 1, b = 30, h = 1$.

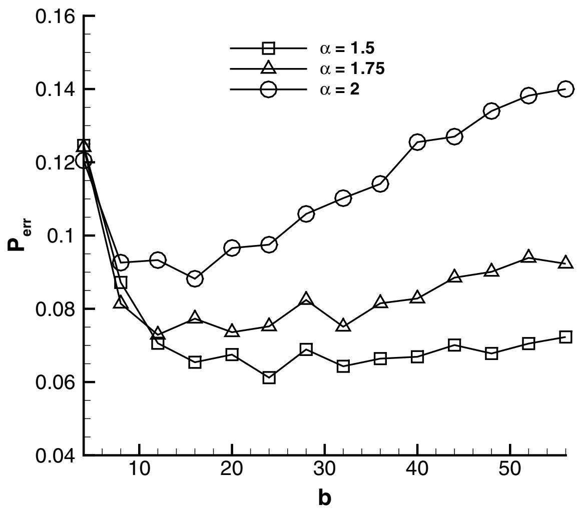

Figure 11. The simulated values of P_{err} versus parameter b with parameters $D = 0.2, a = 1, h = 1, T_b = 1$ s The symbols are data points. The lines are guides to the eye.

We can also simulate the binary signal detection problem according to (15). With the same above parameters, the results are shown in figure 11 and can be found in good agreement to the theoretical results in figure 9.

It is also interesting to note that the ability for the bistable system to detect the binary signal is reduced by the long tailed waiting time, which introduces the time-fractional form of FPE [16]. Theoretically, there exists a critical ratio between the spacial anomalous index and temporal anomalous index, at which the both effects on the detection performance can be cancelled out. The detailed discussions need to be studied in the further work.

4. Conclusion

In this paper, the effects of Lévy noise in aperiodic stochastic resonance have been investigated. Two kinds of aperiodic stochastic resonances, noise-induced ASR and parameter-induced ASR are discussed. The spatial FFPE was numerically solved by the Grünwald–Letnikov implicit finite difference method. It is shown that at every moment during the evolution, the probability distribution density exhibits a sharper distribution with the decrease of Lévy index α. In a binary signal detection problem via a bistable receiver in the presence of Lévy noise, we found that the noise-induced ASR phenomenon still occurs in the presence of Lévy noise, but is reduced by the lower Lévy index α. In the parameter-induced ASR case, with the optimal system parameters, the minimum P_{err} decreased with the decrease of α. Therefore, the performance of the system is improved by Lévy noise compared to Gaussian noise. This anomalous phenomenon may inspire more through investigations in the mechanism of cooperations between the Lévy flights and the external potential.

Acknowledgments

The authors greatly appreciate the support provided by the National Natural Science Foundation of China (key grant number 10332030) and the Foundation of the State Key Laboratory of Fluid Power Transmission and Control.

References

[1] Sahimi M 1998 *Phys. Rep.* **306** 213–395
[2] Hilfer R (ed) 2000 *Applications of Fractional Calculus in Physics* (Singapore: World Scientific)
[3] Metzler R and Klafter J 2000 *Phys. Rep.* **306** 213–395
[4] Mantegna R and Stanley H 2000 *An Introduction to Econophysics Correlations and Complexity in Finance* (Cambridge: Cambridge University Press)
[5] Metzler R and Klafter J 2004 *J. Phys. A: Math. Gen.* **37** R161–208
[6] Chechkin A V, Gonchar V Y, Klafter J and Metzler R 2006 *Adv. Chem. Phys.* **133(B)** 439–96
[7] Benzi R, Sutera A and Vulpiani A 1981 *J. Phys. A: Math. Gen.* **14** L453–7
[8] Gammaitoni L, Hanggi P, Jung P and Marchesoni F 1998 *Rev. Mod. Phys.* **70** 223–87
[9] Wellens T, Shatokhin V and Buchleitner A 2004 *Rep. Prog. Phys.* **67** 45–105
[10] Barbay S, Giacomelli G and Marin F 2000 *Phys. Rev. Lett.* **85** 4652–5
[11] Harmer G P, Davis B R and Abbott D 2002 *IEEE Trans. Instrum. Meas.* **51** 299–309
[12] Xu B, Duan F, Bao R and Li J 2002 *Chaos Solitons Fractals* **13** 633–44
[13] Duan F and Xu B 2003 *Int. J. Bifurcation Chaos* **13** 411–25
[14] Li J and Pan X 2007 *Mech. Syst. Signal Process* **21** 1223–32
[15] Yim M Y and Liu K L 2006 *Physica* A **369** 329–42
[16] Zeng L, Xu B and Li J 2007 *Phys. Lett.* A **361** 455–9
[17] Dybiec B and Gudowska-Nowak E 2006 *Acta Phys. Pol.* B **37** 1479–90
[18] Chechkin A V, Klafter J, Gonchar V Y, Metzler R and Tanatarov L V 2003 *Phys. Rev.* E **67** 10102
[19] Chechkin A V, Gonchar V Y, Klafter J, Metzler R and Tanatarov L V 2004 *J. Stat. Phys.* **115** 1505–35
[20] Fogedby H C 1994 *Phys. Rev. Lett.* **73** 2517–20
[21] Fogedby H C 1998 *Phys. Rev.* E **58** 1690–1712
[22] Feller W 1966 *An Introduction to Probability Theory and its Applications* Vol 1, 2 (New York: Wiley)
[23] Samko S, Kilbas A and Marichev O 1993 *Fractional Integrals and Derivatives - Theory and Applications* (New York: Gordon and Breach)
[24] Podlubny I 1998 *Fractional Differential Equations* (San Diego: Academic)
[25] Gorenflo R, Mainardi F, Moretti D, Pagnini G and Paradisi P 2002 *Chem. Phys.* **284** 521–41
[26] http://economics.sbs.ohio-state.edu/jhm/jhm.html
[27] Jespersen S, Metzler R and Fogedby H C 1999 *Phys. Rev.* E **59** 2736–45
[28] Xu B, Duan F and Chapeau-Blondeau F 2004 *Phys. Rev.* E **69** 61110
[29] Xu B, Li J and Zheng J 2003 *J. Phys. A: Math. Gen.* **36** 11969–80